PHYSICAL REVIEW B **81**, 041313(R) (2010)

Temperature and size-dependent suppression of Auger recombination in quantum-confined lead-salt nanowires

Valery I. Rupasov*
ANTEOS, Inc., Shrewsbury, Massachusetts 01545, USA
(Received 30 November 2009; published 29 January 2010)

Auger recombination (AR) of the ground biexciton state in quantum-confined lead-salt nanowires (NWs) with a strong coupling between the conduction and the valence bands is shown to be strongly suppressed, and only excited biexciton states contribute to Auger decay. The AR rate is predicted to be greatly reduced when temperature or the NW radius are decreased, and the effect is explained by decrease in both the population of excited biexciton states and overlap of phonon-broadened single-exciton and biexciton states. Suppression of AR of multiexciton states exhibiting strong radiative decay makes obviously lead-salt NWs a subject of special interest for numerous lasing applications.

DOI: 10.1103/PhysRevB.81.041313 PACS number(s): 73.21.Hb, 73.22.Dj, 78.67.Lt

Auger recombination (AR) is a nonradiative process, in which the electron-hole recombination energy is transferred to a third charge carrier[1] exciting it to a higher-energy state. In bulk semiconductors, AR is inefficient because of constrains imposed by energy and translational-momentum conservation. But due to relaxation of translation-momentum conservation, the efficiency of Auger-like processes is greatly enhanced in quantum-confined nanocrystals (NCs),[2–4] where AR plays a central role in carrier relaxation.

Effectively one-dimensional nanowires (NWs) occupy an intermediate position between zero-dimensional NCs and bulk materials. In sufficiently long NWs of the length L essentially exceeding the NW radius R, a longitudinal motion of charge carriers along the NW axis is free, while a transverse motion in the plane perpendicular to the NW axis is spatially quantized. The electronic structure of quantum-confined NWs is composed of subbands of the longitudinal motion with a wave vector k, which are also characterized by a spatially quantized wave vector of the transverse motion p. Since electronic transitions between subbands with different p are not forbidden by longitudinal wave-vector conservation, quantum confinement in NWs is expected to result in enhancement of Auger effect compared with bulk parent materials. In particular, Auger decay of the ground biexciton state,[5] which is forbidden in the bulk by energy and translation-momentum conservation, is expected to be allowed in quantum-confined NWs.

A strong coupling between the conduction and the valence bands in lead-salt materials results in significant corrections to the electronic structures of NCs (Ref. 6) and NWs (Ref. 7) computed in the framework of "particle-in-a-box" model[8] not accounting for the interband coupling. However, in the case of NCs, these corrections are mainly quantitative and do not lead to qualitative physical results. In particular, no essential difference is observed in size dependence of AR in narrow-gap NCs and NCs made of wide-gap materials,[4] in which contribution of the interband coupling is relatively small.

But a situation is essentially changed for NWs with a strong interband coupling. In contrast to the case of NCs, the interband coupling in NWs significantly lifts degeneration of low-energy single-particle states of the transverse electron motion resulting in specific selection rules for Auger-like processes. That in its turn leads to qualitative changes in temperature and size behavior of AR compared with those in NCs and bulk materials.

In this Rapid Communication, employing results of our recent studies[7] of the electronic structure of quantum-confined lead-salt NWs, we show that, in sharp contrast to the case of NCs, AR of the ground biexciton state is strongly suppressed, and only excited biexciton states, which are partially populated at finite temperature, contribute to Auger decay of biexcitons. Thus, the total rate of biexciton AR is given by the sum of the rates of excited biexciton states only with conventional weight factors, which determine their population at finite temperature T,

$$W(T,R) = \sum_n W_n(R) e^{-\Delta E_n(R)/T}. \quad (1)$$

Here, size-dependent ΔE_n is the energy difference between nth excited biexciton state with the AR rate W_n and the ground biexciton state. Analytical and numerical computations show that, again in contrast to the case of NCs, size dependence of matrix elements of effective Coulomb coupling for Auger-like processes in NWs is very slow and size dependence of the rates W_n is mainly governed by size-dependent overlap of phonon-broadened single-exciton and biexciton states.

Thus, despite strong spatial quantization of the transverse electron motion resulting in significant relaxation of translation-momentum conservation, temperature and size behavior of AR in NWs qualitatively differ from that in NCs. However, this effect is observed only in NWs with a strong interband coupling, and it is not described in the framework of particle-in-a-box model.

If carrier motions in the conduction and the valence bands are treated as independent of each other, envelope electronic wave functions in the cylindrical coordinate system $(r,\phi,z) \equiv (\boldsymbol{r},z)$ with the Z axis directed along the NW axis are easily found as $\chi_{m_l,s_z} = J_{m_l}(pr) e^{im_l\phi} e^{ikz} \sigma_a$, where J is the Bessel function and $\sigma_a (a = \uparrow, \downarrow)$ are conventional spinors $\sigma_\uparrow = \binom{1}{0}$ and $\sigma_\downarrow = \binom{0}{1}$. Spatially quantized wave vectors of the transverse motion p_n are found from the boundary condition

on the NW interface $r=R$, $J_{m_l}(p_nR)=0$. The quantum states are characterized by the orbital angular momentum projection of the transverse motion on the Z axis $m_l=0,\pm1,\ldots$, the electron spin projection $s_z=\pm\frac{1}{2}$, and continuous wave vector of the longitudinal motion k. Due to mirror symmetry of the conduction and the valence bands, the subband energies E are found to be $\pm\epsilon_{p,k}$ for the conduction (+) and the valence (−) bands, where $\epsilon_{p,k}=(1/2)E_g+(\hbar^2/2m)(p_n^2+k^2)$, E_g is the energy gap, and m is the effective electron mass in both the conduction and the valence bands. The subband states are degenerate with respect to the sign of the orbital angular momentum projection m_l, two possible directions of the electron spin, and two possible directions of the wave vector k. Auger decay of the ground biexciton state is allowed, and the AR rate does not vanish at $T=0$.

In the four-band envelope-function formalism, taking into account a strong coupling between the conduction and the valence bands, total electronic wave functions in lead-salt NCs and NWs are written as a product, $\psi=\Sigma_{i=1}^{i=4}\mathcal{F}_i u_i$, of the four band-edge Bloch functions u_i of the conduction ($i=1,2$) and the valence ($i=3,4$) bands, and four-component envelope functions $\mathcal{F}_i$. The transverse electron motion in NWs is described by bispinors,

$$\Psi_{\pm,m_j}=\frac{1}{\sqrt{4\pi\varepsilon_p}}\begin{pmatrix}\sqrt{\varepsilon_p\pm\epsilon_p}f_{m_l}(r)e^{im_l\phi}\sigma_\uparrow\\ \pm\sqrt{\varepsilon_p\mp\epsilon_p}f_{m_l'}(r)e^{im_l'\phi}\sigma_\downarrow\end{pmatrix} \tag{2a}$$

and

$$\Phi_{\pm,m_j}=\frac{1}{\sqrt{4\pi\varepsilon_p}}\begin{pmatrix}\sqrt{\varepsilon_p\pm\epsilon_p}f_{m_l'}(r)e^{im_l'\phi}\sigma_\downarrow\\ \pm\sqrt{\varepsilon_p\mp\epsilon_p}f_{m_l}(r)e^{im_l\phi}\sigma_\uparrow\end{pmatrix}, \tag{2b}$$

where $m_l=m_j-\frac{1}{2}$, $m_l'=m_j+\frac{1}{2}$, $\epsilon_p=\epsilon_{p,k=0}$, and $\varepsilon_p=\sqrt{\epsilon_p^2+\eta^2p^2}$ is the subband-edge energy, η is a parameter of the interband coupling in lead-salt materials, and $f_{m_l}(r)$ are radial wave functions[7] normalized to unity. The total electronic structure is described by bispinors

$$F_{\pm,m_j}=\frac{1}{\sqrt{2E}}(\sqrt{E\pm\varepsilon}\Psi_{+,m_j}\mp\sqrt{E\mp\varepsilon}\Phi_{-,m_j})\frac{e^{ikz}}{\sqrt{L}} \tag{3a}$$

and

$$G_{\pm,m_j}=\frac{1}{\sqrt{2E}}(\sqrt{E\mp\varepsilon}\Psi_{-,m_j}\pm\sqrt{E\pm\varepsilon}\Phi_{+,m_j})\frac{e^{ikz}}{\sqrt{L}} \tag{3b}$$

in the conduction (+) band with the eigenenergy $E=+\sqrt{\epsilon_{p,k}^2+\eta^2(p^2+k^2)}$, and in the valence (−) band with the eigenenergy $-E$, where $\varepsilon=\sqrt{\epsilon_{p,k}^2+\eta^2p^2}$. Electronic subbands are characterized by the total angular momentum projection $m_j=m_l+s_z=\pm\frac{1}{2},\pm\frac{3}{2},\ldots$ on the Z axis and the wave vector of longitudinal motion k.

Two distinct sets of spatially quantized wave vectors of the transverse motion p_n and q_n ($n=0,1,\ldots$) are found from boundary condition equations

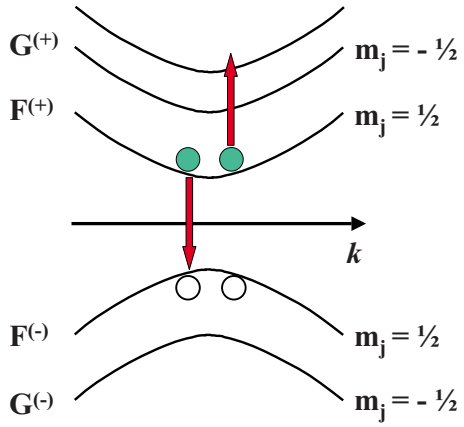

FIG. 1. (Color online) Subbands of the longitudinal electron motion in NWs with the strong interband coupling.

$$\frac{\sqrt{\varepsilon_p+\epsilon_p}}{\sqrt{\epsilon_\lambda-\varepsilon_p}}\frac{J_{m_j-1/2}(pR)}{I_{m_j-1/2}(\lambda R)}=\frac{\sqrt{\varepsilon_p-\epsilon_p}}{\sqrt{\epsilon_\lambda+\varepsilon_p}}\frac{J_{m_j+1/2}(pR)}{I_{m_j+1/2}(\lambda R)} \tag{4a}$$

for the bispinors Ψ_+ and Φ_- and

$$\frac{\sqrt{\varepsilon_p+\epsilon_q}}{\sqrt{\epsilon_\lambda-\varepsilon_p}}\frac{J_{m_j+1/2}(qR)}{I_{m_j+1/2}(\lambda R)}=\frac{\sqrt{\varepsilon_p-\epsilon_q}}{\sqrt{\epsilon_\lambda+\varepsilon_p}}\frac{J_{m_j-1/2}(qR)}{I_{m_j-1/2}(\lambda R)} \tag{4b}$$

for the bispinors Ψ_- and Φ_+, where $\lambda=\sqrt{p^2+\lambda_0^2}$, $\lambda_0=2m/\hbar^2\sqrt{(\hbar^2/2m)E_g+\eta^2}$, and $\epsilon_\lambda=\epsilon_{p,k=0}+2m/\hbar^2\eta^2$. Since the longitudinal motion mixes Ψ_+ and Φ_- bispinors in bispinors F and Ψ_- and Φ_+ bispinors in bispinors G, Eqs. (4a) and (4b) determine spatially quantized wave vectors p_n and q_n for F and G subbands, respectively. Thus, the interband coupling completely lifts degeneration of transverse motion states, and subband states in a given L valley are degenerate with respect to two possible directions of the wave vector k only.

In terms of envelope functions, a matrix element of long-range Auger process in the conduction band for the ground biexciton state, shown in Fig. 1, is derived as

$$\Gamma_g=\int d\boldsymbol{r}_1d\boldsymbol{r}_2[F_{-,1/2}^\dagger(\boldsymbol{r}_1)\mathcal{F}_{+,m_j}^\dagger(\boldsymbol{r}_2)-\mathcal{F}_{+,m_j}^\dagger(\boldsymbol{r}_1)F_{-,1/2}^\dagger(\boldsymbol{r}_2)]\times\mathcal{U}(\boldsymbol{r}_1,\boldsymbol{r}_2)F_{+,1/2}(\boldsymbol{r}_2)F_{+,1/2}(\boldsymbol{r}_1), \tag{5}$$

where the wave functions of the longitudinal motion $\frac{1}{\sqrt{L}}e^{ikz}$ are included into an effective Coulomb coupling

$$\mathcal{U}(\boldsymbol{r}_1,\boldsymbol{r}_2)=\frac{1}{L^2}\int_0^L dz_1dz_2U(\boldsymbol{r}_1,z_1;\boldsymbol{r}_2,z_2)\times\exp\{i[(k_1-k_1')z_1+(k_2-k_2')z_2]\},$$

which does not depend on R at small $\Delta k=|k_1-k_1'|=|k_2-k_2'|\ll R^{-1}$. Here U is the energy of both direct Coulomb coupling and interparticle coupling via medium polarization. Owing to conservation of the total angular momentum projection, an electron in the conduction band can be excited only to subbands with $m_j=\frac{1}{2}$.

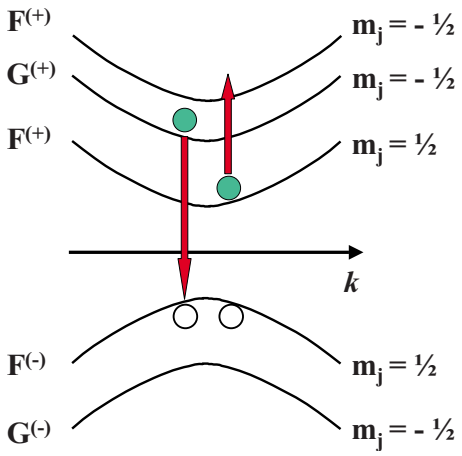

FIG. 2. (Color online) Auger recombination of the first excited biexciton state, in which one of electrons is in the subband $G_{+,-1/2}$.

Nearby subband edges, where the energy differences $E-\varepsilon$ in Eqs. (3) are small, the expressions for F and G bispinors are simplified,

$$F_+ \simeq \Psi_+ - \rho\Phi_-, \quad F_- \simeq \rho\Psi_+ + \Phi_-,$$

$$G_+ \simeq \rho\Psi_- + \Phi_+, \quad G_- \simeq \Psi_- - \rho\Phi_+,$$

where $\rho = \eta k/2\varepsilon_0$ is the ratio of the longitudinal interband coupling energy to the energy of the transverse motion. In PbSe material, the parameter of interband coupling $\eta \simeq 0.31$ eV nm (Ref. 6) and at small $k \sim 2\pi/L$ and $L \sim 10$ μm, the parameter ρ is estimated to be of the order of $(2-5)\times 10^{-4}$ for PbSe NWs of the radius of 2–8 nm.

Due to orthogonality of the spinors σ_a, $\sigma_\uparrow^\dagger \cdot \sigma_\downarrow = 0$, Ψ and Φ bispinors are also orthogonal to each other, $\Psi_{m_j}^\dagger \cdot \Phi_{m_j'} = 0$. Therefore, a contribution of recombination process for an electron from F_+ subband and a hole from F_- subband to the matrix element Γ_g is proportional to ρ. Correspondingly, the contribution to the AR rate $W_g \sim \Gamma_g^2$ is of the order of $\rho^2 \sim 10^{-7}$, i.e., AR of the ground biexciton state is strongly suppressed.

In general, we derive the following selection rules for Auger-like processes valid for states with sufficiently small wave vectors of the longitudinal motion.

(i) Electron-hole recombination is allowed (i.e., it does not bring the small factor ρ into a matrix element of Auger-like process) only if an electron and a hole belong to different subbands: F_+ and G_- or G_+ and F_-.

(ii) On the contrary, electronic intraband transitions are allowed only inside F and G manifolds since a transition, in which an electron is transferred from $F(G)$ to $G(F)$ subband inside the conduction (valence) band, brings the small factor ρ into a matrix element of the process.

The first excited biexciton states are constructed from the ground state if one of electrons (holes) is transferred to the subband $G_{+,-1/2}(G_{-,-1/2})$, and the expression for matrix element of Auger decay of the excited biexciton state illustrated in Fig. 2 is derived as

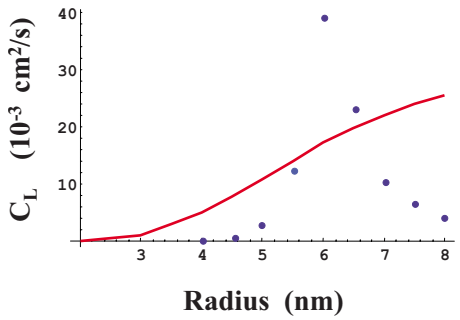

FIG. 3. (Color online) Size dependence of the linear AR coefficients C_{L_1} (curve) and C_{L_2} (solid circles) in PbSe NWs of the radius of 2–8 nm.

$$\Gamma_n = \int d\boldsymbol{r}_1 d\boldsymbol{r}_2 F_{-,1/2}^\dagger(\boldsymbol{r}_1) F_{+,-1/2}^\dagger(\boldsymbol{r}_2, p_n) \mathcal{U}(\boldsymbol{r}_1, \boldsymbol{r}_2) \times F_{+,1/2}(\boldsymbol{r}_2) G_{+,-1/2}(\boldsymbol{r}_1), \tag{6}$$

where $n=1,2,\ldots$ numerates the spatially quantized wave vectors of the transverse motion p_n of the excited electron or, in other words, subbands $F_{+,-1/2}$ with different wave vectors p_n. Now recombination of G electron and F hole is allowed by the selection rules. To conserve the total angular momentum projection an electron is excited to F subbands with $m_j = -\frac{1}{2}$, since a transition to G subbands brings the small factor ρ. Then, summarizing over all channels of Auger decay of the first excited biexciton states, we derive for the AR rate to the second order of perturbation theory

$$W(T,R) = \frac{16\pi}{\hbar} e^{-\Delta E/T} \sum_n D(\delta E_n) \Gamma_n^2, \tag{7a}$$

where the function D describes overlap of the phonon-broadened final single-exciton state of the energy E_x and initial biexciton states of the energy E_{xx} with the energy detuning $\delta E = E_{xx} - E_x$.

Since at present we do not have any dependable experimental data on shapes, characteristic widths and Stokes shifts of phonon-broadened electronic states in NWs, we use for the function D a simplified integral form $D(\delta E) = \int g(E) g(E - \delta E) dE$, assuming, as in Ref. 9, that the function $g(E)$ is the Lorentzian with the width γ and the Stokes shift Λ. Then, we finally find

$$W(T,R) = \frac{16}{\hbar} e^{-\Delta E/T} \sum_n \frac{\gamma}{(\delta E_n - 2\Lambda)^2 + \gamma^2} \Gamma_n^2. \tag{7b}$$

To characterize the AR efficiency for multiexciton states, we introduce a "linear" length-independent AR coefficient $C_L = WL^2$, which is analogous to the AR coefficient in bulk materials. Then, the AR time of multiexciton states is found as $\tau = (C_L n_L^2)^{-1}$, where n_L is the linear density of excitons.

The results of numerical calculations of the linear coefficient C_L with $\gamma = 20$ meV and $\Lambda = 50$ meV for PbSe NWs of the radius of 2–8 nm at $T = 300$ K are presented in Fig. 3. The total coefficient is the sum of coefficients C_{L_1} and C_{L_2},

which correspond to AR processes with an electron excitation to subbands with the wave vectors p_1 and p_2, respectively.

Although numerical calculations are quite sensitive to unknown parameters of electron-phonon coupling, the obtained results demonstrate basic trends in temperature and size behavior of the AR efficiency in NWs.

The matrix elements Γ_1 and Γ_2 depend on the NW radius very slowly, and size dependence of the AR efficiency is mainly governed by size-dependent overlap of phonon-broadened single-exciton and biexciton states. Therefore, size dependence of the AR efficiency in NWs is reverse to that in NCs: it is greatly reduced with decreasing R, while in NCs, size dependence is mainly governed by size-dependent matrix elements of Coulomb coupling ($\propto R^{-1}$), and the AR rate scales as R^{-3}.[3,4]

The coefficient C_{L_2} exhibits a strong resonance behavior due to vanishing $\delta E_2 - 2\Lambda$ at the radius of about 6 nm, where the phonon-broadened single-exciton and biexciton states are well overlap each other.[10] Despite Γ_2 is much smaller Γ_1, $\Gamma_2 \simeq 0.1\Gamma_1$, a contribution of the resonance channel to the total coefficient C_L exceeds nearby resonance a contribution of the nonresonance channel, in which $\delta E_1 - 2\Lambda \gg \gamma$ at all NW radii.

To compare AR efficiencies in NWs and bulk parent materials, it is illustrative to introduce a "volume" coefficient $C_V = C_L S^2$, where S is the NW cross-section area. The AR coefficient C_{bulk} in bulk PbSe was measured[11] to be approximately constant between 300 and 70 K with a value of about 8×10^{-28} cm^6/s and then drops a value of about 1×10^{-28} cm^6/s at $T=30$ K. The huge growth of the volume coefficient C_V in NWs from 2.2×10^{-30} ($R=2$ nm, strongly suppressed AR) to 1.2×10^{-25} cm^6/s ($R=8$ nm, greatly enhanced AR) is determined by increasing both the linear coefficient C_L in a wide interval from 0.14×10^{-3}($R=2$ nm) to 30×10^{-3} cm^2/s($R=8$ nm) and the NW volume.

It is easy to see that AR in NWs demonstrates a qualitatively different temperature behavior compared with that in bulk parent material: AR in NWs is temperature suppressed due to decreasing the population of excited biexciton states, which scales as $e^{-\Delta E_n/T}$, where ΔE_1 for the first excited biexciton states ranges in the interval from 117 meV ($R=2$ nm) to 13 meV ($R=8$ nm).

Overall, we have shown that owing to specific selection rules for Auger-like processes in lead-salt NWs with a strong coupling between the conduction and the valence bands, AR is strongly suppressed in "slim" NWs of the radius $R<4$ nm($C_V \ll C_{\text{bulk}}$), but significantly enhanced ($C_V \gg C_{\text{bulk}}$) at $R>4$ nm in comparison with bulk PbSe material. Moreover, temperature dependence qualitatively differs from that in bulk parent material and NCs. Finally, size dependence is reversed to that in NCs: the AR rate is greatly reduced with decreasing the NW radius, while in NCs it grows as R^{-3}.

Ultrafast multiexciton decay via AR is a major impediment for prospective applications of semiconductor NCs in lasing.[4] Therefore, suppression of AR of the ground biexciton state exhibiting strong radiative decay of electron-hole pairs with the dipole momentum mainly determined by the longitudinal Kane momentum of bulk material makes obviously quantum-confined lead-salt NWs a subject of special interest for numerous lasing applications in near-infrared and mid-infrared spectral ranges.

I would like to thank Victor Klimov for numerous helpful discussions and remarks.

*valery_rupasov@hotmail.com

[1] P. T. Landsberg, *Recombination in Semiconductors* (Cambridge University Press, Cambridge, 1991).

[2] D. I. Chepic, Al. L. Efros, A. I. Ekimov, M. G. Ivanov, V. A. Kharchenko, L. A. Kudriavtsev, and T. V. Yazeva, J. Lumin. **47**, 113 (1990).

[3] V. I. Klimov, A. A. Mikhailovsky, D. W. McBranch, C. A. Leatherdale, and M. G. Bawendi, Science **287**, 1011 (2000).

[4] V. I. Klimov, Annu. Rev. Phys. Chem. **58**, 635 (2007).

[5] For simplicity, we use the term "exciton" for an electron-hole pair in a NW and do not account in this Rapid Communication for bound electron-hole states (Ref. 7).

[6] I. Kang and F. W. Wise, J. Opt. Soc. Am. B **14**, 1632 (1997).

[7] V. I. Rupasov, Phys. Rev. B **80**, 115306 (2009).

[8] Al. L. Efros and M. Rosen, Annu. Rev. Mater. Sci. **30**, 475 (2000).

[9] L.-W. Wang, M. Califano, A. Zunger, and A. Franceschetti, Phys. Rev. Lett. **91**, 056404 (2003).

[10] An analogous size-dependent resonance between single-exciton and biexciton states in PbSe NCs has been employed by A. Shabaev, A. Efros, and A. Nozik, Nano Lett. **6**, 2856 (2006) to explain the carrier multiplication effect in NCs [R. D. Schaller and V. I. Klimov, Phys. Rev. Lett. **92**, 186601 (2004); see, for a review, Ref. 4] However, the resonance in the AR rate is not observed in experiments with NCs of the radius of 2–6 nm, that can be attributed to large values of the Stokes shifts of high-energy states. For the same reason, the resonance term in the AR rate in NWs can be shifted to larger radii at greater values of Stokes shifts.

[11] P. C. Findlay, C. R. Pidgeon, R. Kotitschke, A. Hollingworth, B. N. Murdin, C. J. G. M. Langerak, A. F. G. van der Meer, C. M. Ciesla, J. Oswald, A. Homer, G. Springholz, and G. Bauer, Phys. Rev. B **58**, 12908 (1998).